

## Research Article

# The Role of Constraints in a Segregation Model: The Asymmetric Case

**Davide Radi,<sup>1</sup> Laura Gardini,<sup>2</sup> and Viktor Avrutin<sup>2,3</sup>**

<sup>1</sup> *Department of Management, Polytechnic University of Marche, 60121 Ancona, Italy*

<sup>2</sup> *DESP, University of Urbino "Carlo Bo," 61029 Urbino, Italy*

<sup>3</sup> *IST, University of Stuttgart, 70569 Stuttgart, Germany*

Correspondence should be addressed to Davide Radi; [d.radi@univpm.it](mailto:d.radi@univpm.it)

Received 22 May 2014; Accepted 29 July 2014; Published 31 August 2014

Academic Editor: Daniele Fournier-Prunaret

Copyright © 2014 Davide Radi et al. This is an open access article distributed under the Creative Commons Attribution License, which permits unrestricted use, distribution, and reproduction in any medium, provided the original work is properly cited.

We extend the analysis on the effects of the entry constraints on the dynamics of an adaptive segregation model of Shelling's type when the two populations involved differ in numerosity, level of tolerance toward members of the other population, and speed of reaction. The model is described by a two-dimensional piecewise smooth dynamical system in discrete time, where the entry constraints represent possible exogenous controls imposed by an authority in order to regulate the maximum number of members of the two populations allowed to enter the system, usually the district in which they live in. In this paper, we investigate the nature of some particular border collision bifurcations and discuss the policy implications of the entry constraints in terms of segregation. The investigation reveals that asymmetries in the level of tolerance of the two populations involved may lead to phenomena of overreaction or overshooting in the adjustment process. In order to avoid the risk of segregation, suitable entry limitations must be imposed at least on the more tolerant population.

## 1. Introduction

In the modern economic world, with flows of workers from country to country, (residential) segregation represents one of the main socioeconomic concerns for the public authorities. In the past, the problem regarded mainly the cities in the USA; see, for example, [1]. In the last two decades, segregation has become one of the main public economic issues also in all Western-European countries. The open borders policies of the European Union facilitate the migration from country to country of people of different nationalities, languages, skills, and cultures. This process raises the necessity of integration between the indigenous dwellers and the newcomers.

The main force that prevents integration between members of different groups is the limited tolerance of members of one group towards members of other groups. Aware of this, the policymakers tend to avoid segregation by combining some integration policies mainly focused to promote multiculturalism; see, for example, [2], with more drastic measures such as the imposition of some entry constraints

for the members of the different groups. Although possible effects of this strategy are still not completely investigated, this last solution is often adopted by public authorities as it is the one that generates results in a short period.

In this paper, by means of an adaptive segregation model of Shelling's type, as proposed in [3] and formalized in a mathematical model in [4], we study the effectiveness of entry constraints in preventing segregation. The model is a simplified representation of a real world situation in which there are two groups of people which differ in some respects, such as, color of skin, religion, and political affiliation. Each single member of each group has a different and limited level of tolerance on the maximum number of people of the other group living in the same system, where system commonly refers to a "district" of a city. This model captures the relevant mismatch between individual preferences, which would exclude segregation, and collective pattern that results from the interplay of individual choices, which often lead to segregation, see [5]. The validity of this theoretical finding has been confirmed, mainly through empirical surveys, by many

scholars; see for example, [1, 6–8]. This aspect is not only a peculiarity of the issue described here but is typical of all socioeconomic systems that the willingness of the individuals is not reflected in the collective choice.

The dynamical analysis of the model is conducted with the aim of understanding the possible consequences of imposing more or less stringent entry constraints in terms of segregation. The investigation reveals that, to avoid segregation, it is good to impose entry constraints on the more tolerant population as this reduces the risk of overshooting or over-reaction among agents of the two groups and leads to an equilibrium of coexistence. The finding is of particular interest as it runs counter to common opinion that, to avoid segregation, we have to limit entrances of the less tolerant population and reveals that policymakers should impose the entry constraints for the different groups involved in a system in such a way to balance the entries of the members of each group into the system if they want to prevent segregation.

The analysis conducted in the paper is also devoted to show the different dynamical scenarios that can occur for different values of the entry constraints. In particular, an accurate bifurcation analysis highlights the existence of interesting border collision bifurcations which lead to the transition from a stable fixed point to cycles of different periodicity and chaotic attractors. The mathematical analysis makes use of the last developments on the bifurcation theory of nonsmooth dynamical system in discrete time; see, for example, [9–12], to provide a full and comprehensive description of the complex dynamics that comes out of the original model of segregation of Schelling. The dynamics of the system are particularly interesting from a mathematical point of view as the model is described by a continuous two-dimensional piecewise differentiable map characterized by several borders through which the system changes its definition. It is worth remarking that the dynamics associated with piecewise smooth systems is a quite new research branch, and several papers have been dedicated to this subject in the last decade; see for example, [13, 14]. Such an increasing interest towards nonsmooth dynamics comes both from the new theoretical problems occurring due to the presence of borders and from the wide interest in the applied context. In fact, many models are described by constrained functions, leading to piecewise smooth systems, continuous or discontinuous. We recall several oligopoly models with different kinds of constraints considered in the books [15, 16], nonsmooth economic models in [17–19], financial market models in [20–22], and multiple-choice models in [23–25].

This paper extends and generalizes the results in [26] to asymmetric cases, where the two populations involved in the system differ in terms of number of members, maximum level of tolerance of members of the other group, and speed of reaction to differences between the maximum tolerated number of members of the other group and their effective presence in the system. The analysis conducted here is of particular interest as in reality the groups of people that are involved in the system differ in at least one of the three mentioned aspects. The investigation of the dynamics of the segregation model for an asymmetric setting of the parameters reveals

that new type of bifurcations can occur with respect to the symmetric case studied in [26].

The paper is organized as follows. In Section 2, we introduce the model and we indicate its fixed points. In Section 3, we provide a deep investigation of the main dynamics generated by the model and the possible scenarios for different parameters' values, and we discuss the findings in terms of policy implications. In Section 4, we conclude and provide some possible future extensions and improvements of the model.

## 2. The Segregation Model and Its Peculiarities

We consider the Segregation Model as originally proposed by Schelling, formalized in [4] and considered also in [26]:

$$\begin{aligned} (x_1(t+1), x_2(t+1)) \\ &= T(x_1(t), x_2(t)) \\ &= (T_1(x_1(t), x_2(t)), T_2(x_1(t), x_2(t))) \end{aligned} \quad (1)$$

with

$$\begin{aligned} T_1(x_1, x_2) &= \begin{cases} 0 & \text{if } F_1(x_1, x_2) \leq 0 \\ F_1(x_1, x_2) & \text{if } 0 \leq F_1(x_1, x_2) \leq K_1 \\ K_1 & \text{if } F_1(x_1, x_2) \geq K_1 \end{cases} \\ T_2(x_1, x_2) &= \begin{cases} 0 & \text{if } F_2(x_1, x_2) \leq 0 \\ F_2(x_1, x_2) & \text{if } 0 \leq F_2(x_1, x_2) \leq K_2 \\ K_2 & \text{if } F_2(x_1, x_2) \geq K_2, \end{cases} \end{aligned} \quad (2)$$

where

$$\begin{aligned} F_1(x_1, x_2) &= x_1 [1 - \gamma_1 x_2 + \gamma_1 x_1 R_1(x_1)], \\ F_2(x_1, x_2) &= x_2 [1 - \gamma_2 x_1 + \gamma_2 x_2 R_2(x_2)], \\ R_i(x_i) &= \tau_i \left( 1 - \frac{x_i}{N_i} \right), \quad i = 1, 2. \end{aligned} \quad (3)$$

In (1)–(3),  $\gamma_i$ ,  $\tau_i$ ,  $N_i$ ,  $K_i$  are positive constants and  $K_i \leq N_i$  for  $i = 1, 2$ . The state variables  $x_1(t)$  and  $x_2(t)$  give the numbers of members of populations 1 and 2, respectively, that are in the system in period  $t$ . The total number of members of population  $i$  is  $N_i$ . The functions  $x_i R_i(x_i)$ ,  $i = 1, 2$ , indicate the maximum number of members of the other population tolerated by  $x_i$  members of population  $i$ . The parameter  $\tau_i$  measures the level of tolerance of population  $i$ . The entry and exit decisions are modelled by an adaptive dynamics indicated by the functions  $F_i$ . Indeed, by definition of  $F_i$ , we have that the number of members of population  $i$  that decide to enter (or exit) the system at each iteration is simply given by the difference between the maximum tolerated number of members of the other group and the number of agents of the other group that are in the system; that is,  $\gamma_i x_i [x_i R_i(x_i) - x_j]$ , where  $\gamma_i$  is a parameter measuring the speed of adjustment. The parameter  $K_i$  represents the entry constraint indicating the maximum number of members of population  $i$  allowed to enter the system. The smaller the values of these two parameters, the more stringent are the entry constraints.

From the definition of the map, we have that the phase plane of the dynamical system can be divided into several regions where the system is defined by different functions. On the boundaries of these regions, the map is continuous but not differentiable.

The boundaries of non differentiability are given by the curves  $F_i(x_1, x_2) = K_i$ , which can be written in explicit form as follows:

$$\begin{aligned} BC_{1,K} : x_2 &= \frac{[1 + \gamma_1 x_1 R_1(x_1) - (K_1/x_1)]}{\gamma_1}, \\ &\text{where } F_1(x_1, x_2) = K_1, \\ BC_{2,K} : x_1 &= \frac{[1 + \gamma_2 x_2 R_2(x_2) - (K_2/x_2)]}{\gamma_2}, \\ &\text{where } F_2(x_1, x_2) = K_2 \end{aligned} \quad (4)$$

and the solutions of  $F_i(x_1, x_2) = 0$  which, as it is immediate, are satisfied by  $x_i = 0$ , and other points belonging to the curves given by

$$\begin{aligned} BC_{1,0} : x_2 &= \frac{[1 + \gamma_1 x_1 R_1(x_1)]}{\gamma_1}, \\ &\text{where } F_1(x_1, x_2) = 0, \quad x_1 \neq 0, \\ BC_{2,0} : x_1 &= \frac{[1 + \gamma_2 x_2 R_2(x_2)]}{\gamma_2}, \\ &\text{where } F_2(x_1, x_2) = 0, \quad x_2 \neq 0. \end{aligned} \quad (5)$$

These curves of nondifferentiability divide the phase plane into the following nine regions:

$$\begin{aligned} \Omega_1 &= \{(x_1, x_2) \mid 0 \leq F_1(x_1, x_2) \leq K_1, 0 \leq F_2(x_1, x_2) \leq K_2\}, \\ \Omega_2 &= \{(x_1, x_2) \mid F_1(x_1, x_2) \leq 0, 0 \leq F_2(x_1, x_2) \leq K_2\}, \\ \Omega_3 &= \{(x_1, x_2) \mid F_1(x_1, x_2) \leq 0, F_2(x_1, x_2) \leq 0\}, \\ \Omega_4 &= \{(x_1, x_2) \mid F_1(x_1, x_2) \leq 0, F_2(x_1, x_2) \geq K_2\}, \\ \Omega_5 &= \{(x_1, x_2) \mid F_1(x_1, x_2) \geq K_1, 0 \leq F_2(x_1, x_2) \leq K_2\}, \\ \Omega_6 &= \{(x_1, x_2) \mid F_1(x_1, x_2) \geq K_1, F_2(x_1, x_2) \leq 0\}, \\ \Omega_7 &= \{(x_1, x_2) \mid F_1(x_1, x_2) \geq K_1, F_2(x_1, x_2) \geq K_2\}, \\ \Omega_8 &= \{(x_1, x_2) \mid 0 \leq F_1(x_1, x_2) \leq K_1, F_2(x_1, x_2) \leq 0\}, \\ \Omega_9 &= \{(x_1, x_2) \mid 0 \leq F_1(x_1, x_2) \leq K_1, F_2(x_1, x_2) \geq K_2\} \end{aligned} \quad (6)$$

in each of which a different function is to be applied, so that we have

$$\begin{aligned} (x_1, x_2) \in \Omega_1 : (x'_1, x'_2) &= (F_1(x_1, x_2), F_2(x_1, x_2)), \\ (x_1, x_2) \in \Omega_2 : (x'_1, x'_2) &= (0, F_2(x_1, x_2)), \\ (x_1, x_2) \in \Omega_3 : (x'_1, x'_2) &= (0, 0), \end{aligned}$$

$$\begin{aligned} (x_1, x_2) \in \Omega_4 : (x'_1, x'_2) &= (0, K_2), \\ (x_1, x_2) \in \Omega_5 : (x'_1, x'_2) &= (K_1, F_2(x_1, x_2)), \\ (x_1, x_2) \in \Omega_6 : (x'_1, x'_2) &= (K_1, 0), \\ (x_1, x_2) \in \Omega_7 : (x'_1, x'_2) &= (K_1, K_2), \\ (x_1, x_2) \in \Omega_8 : (x'_1, x'_2) &= (F_1(x_1, x_2), 0), \\ (x_1, x_2) \in \Omega_9 : (x'_1, x'_2) &= (F_1(x_1, x_2), K_2) \end{aligned} \quad (7)$$

and, as already remarked, the map is continuous: on a border between two different regions the applied functions take the same value.

From the definition of map  $T$  in (1), it follows immediately that the rectangle

$$D = [0, K_1] \times [0, K_2] \quad (8)$$

is absorbing, as any point of the plane is mapped in  $D$  in one iteration and an orbit cannot escape from it. Thus,  $D$  is our region of interest. In general, depending on the values of the parameters, only a few of the regions  $\Omega_j$  for  $j = 1, \dots, 9$  may have a portion, or subregion, present in  $D$ , say  $\Omega_j \cap D \neq \emptyset$ , as shown, for example, in Figure 1(a). In any case, the behavior of the map in the other regions, not entering  $D$ , may be easily explained. To this purpose, let us first recall from [26] a few remarks on the fixed points that the system can have.

The fixed points of the system, satisfying  $T(x_1, x_2) = (x_1, x_2)$ , are associated with the solutions of several equations. We can distinguish between “*fixed points of segregation*” and “*fixed points of non segregation*” when the two kinds of populations coexist. A fixed point of the first kind is a point on one axis, which corresponds to disappearance (i.e., extinction) of one population. Since the axes are invariant, that is,  $T(x_1, 0) = (T_1(x_1, 0), T_2(x_1, 0)) = (T_1(x_1, 0), 0)$  and  $T(0, x_2) = (T_1(0, x_2), T_2(0, x_2)) = (0, T_2(0, x_2))$ , the fixed points of segregation solve either  $\bar{x}_1 = T(\bar{x}_1, 0)$  or  $\bar{x}_2 = T(0, \bar{x}_2)$ . From this, we have that  $(K_1, 0)$  and  $(0, K_2)$  are two equilibria of segregation which are feasible for  $K_1 \leq N_1$  and  $K_2 \leq N_2$ , respectively. Considering the restriction of the map  $T$  to the axes, it is straightforward to prove that the equilibria of segregations  $(K_1, 0)$  and  $(0, K_2)$  are always superstable (we recall that a superstable cycle of a one-dimensional map is a cycle with eigenvalue zero, for a two-dimensional map it is a cycle with two eigenvalues zero) for the restriction. We note that  $(0, 0)$  is also a fixed point of the model, which can be defined as “*equilibrium of extinction*,” as it represents a situation in which all the members of the two populations decide to leave the system. Concerning the “*fixed points of non segregation*,” it is worth distinguishing between “*natural fixed points of non segregation*” and “*artificial fixed points of non segregation*.” The first ones are all the admissible solutions of

$$\begin{aligned} x_1 R_1(x_1) &= x_2, \\ x_2 R_2(x_2) &= x_1. \end{aligned} \quad (9)$$

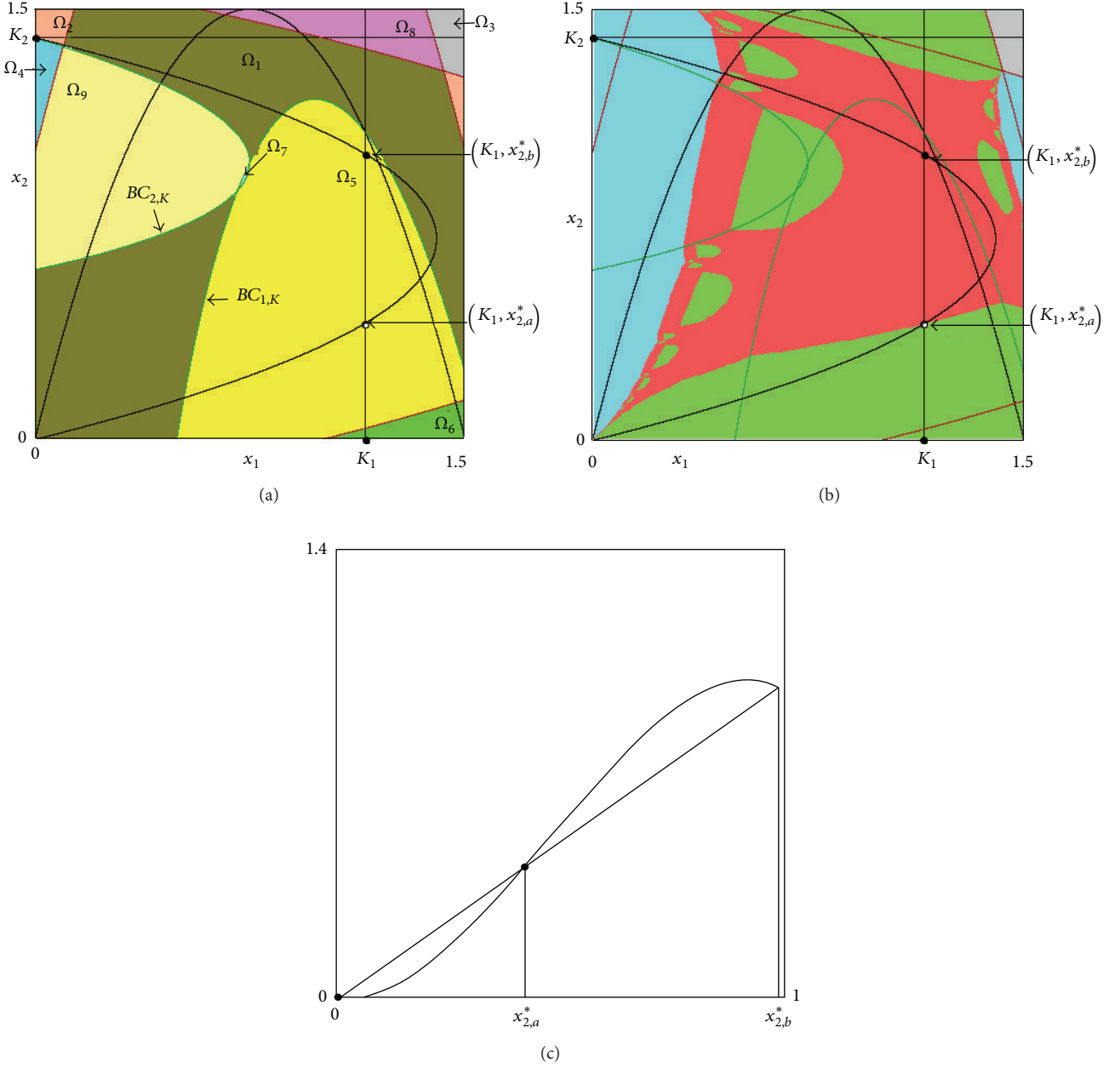


FIGURE 1: Parameters:  $N_1 = 1.5$ ,  $N_2 = 1.4$ ,  $\tau_1 = \tau_2 = 4$ ,  $\gamma_1 = \gamma_2 = 1$ ,  $K_1 = 1.15$ , and  $K_2 = 1.4$ . Panel (a), phase space divided in regions  $\Omega_i$ ,  $i = 1, \dots, 9$ . Panel (b), the green (resp., azure) region is the basin of attraction of the superstable equilibrium of segregation  $(K_1, 0)$  (resp.,  $(0, K_2)$ ), and the red region is the basin of attraction of the equilibrium of nonsegregation  $(K_1, x_{2,b}^*)$ . In the first two Panels,  $BC_{1,K}$  and  $BC_{2,K}$  are the dark-green curves and  $BC_{1,0}$  and  $BC_{2,0}$  the dark-red curves, while  $\phi_1$  and  $\phi_2$  are the black curves. Panel (c), graph of the restriction of the map  $T$  on  $x_1 = K_1$  for  $x_2 \in [0, x_{2,m}]$ .

In the phase plane, they are given by the intersection points of the two reaction curves:

$$\phi_1 : x_2 = x_1 R_1(x_1), \quad \phi_2 : x_1 = x_2 R_2(x_2). \quad (10)$$

The label “*natural fixed points of non segregation*” makes it clear that these fixed points exist without imposing entry constraints. These fixed points are feasible or admissible if and only if they belong to the region  $\Omega_1 \cap D$ ; otherwise, they are called virtual.

We call “*artificial fixed points of non segregation*” those which would not exist without imposing entry constraints. An example is the point  $(K_1, K_2)$  if it belongs to the region  $\Omega_7 \cap D$  and of the same kind are the intersection points of the horizontal straight line  $x_1 = K_1$  and  $\phi_2$ , say  $(K_1, x_{2,a}^*)$  and  $(K_1, x_{2,b}^*)$ , with  $x_{2,a}^*$  and  $x_{2,b}^*$  solving  $x_2 R_2(x_2) = K_1$ , when they belong to the region  $\Omega_5 \cap D$ ; otherwise, they are virtual. Similarly, we can consider the intersection points of the horizontal straight line  $x_2 = K_2$  and  $\phi_1$  leading to



the fixed points  $(x_{1,a}^*, K_2)$  and  $(x_{1,b}^*, K_2)$ , with  $x_{1,a}^*$  and  $x_{1,b}^*$  solving  $x_1 R(x_1) = K_2$ , when they belong to the region  $\Omega_9 \cap D$ .

The segregation model has some peculiarities, due to the different definitions of the map in the several regions  $\Omega_j$ , which may lead to different kinds of degeneracy. For example, when a portion of the region  $\Omega_7$  exists in  $D$ , then all the points of that region are mapped into a unique point: the corner point  $P = (K_1, K_2)$  of the absorbing rectangle  $D$ , which means that, in the region  $\Omega_7$ , we have two eigenvalues equal to zero in the Jacobian matrix at any point of  $\Omega_7$ . Thus, when the point  $P$  belongs to  $\Omega_7 \cap D$  then it is a superstable fixed point. While when  $P$  does not belong to  $\Omega_7 \cap D$ , then for the dynamics of the points in region  $\Omega_7$  it is enough to consider the trajectory of the only point  $P$ .

Other regions with degeneracies are  $\Omega_3$ ,  $\Omega_4$ , and  $\Omega_6$  as all of them are mapped into fixed points,  $(0, 0)$ ,  $(0, K_2)$ , and  $(K_1, 0)$ , respectively. These fixed points do not deserve other comments apart from their local stability/instability. The *equilibrium of extinction* is unstable while the two other *fixed points of segregation* are superstable when  $\Omega_4$  and  $\Omega_6$  intersect  $D$  in a set of positive measure, stable otherwise.

There are other degeneracies of the map, due to the regions bounded by the border curves  $BC_{i,K}$  (see Figure 1(a)). The portion of the phase plane bounded by the border curve  $BC_{1,K}$  is mapped onto the line  $x_1 = K_1$ . Similarly the whole region bounded by the border curve  $BC_{2,K}$  is mapped onto the line  $x_2 = K_2$ . Thus, in both regions we have one degeneracy as the Jacobian matrix in all the points of these regions has one eigenvalue equal to zero. As a whole region is mapped into a segment of straight line, the stability/instability of the fixed points belonging to these lines, which are the *artificial fixed points of nonsegregation*, can be investigated considering the one-dimensional restriction of  $T$  to the lines (when they are real fixed points of  $T$  and not virtual). As we shall comment in the next section, an example is shown in Figures 1(b) and 1(c).

Summarizing, besides the natural fixed point of nonsegregation satisfying the equations in (13), which may be real (stable or unstable) or virtual, we list below those which can be considered the principal fixed points of the constrained model, although other fixed points may exist, depending on the values of the parameters (for example in the piecewise smooth maps of the restrictions on the lines  $x_i = K_i$ ).

- $(0, 0)$ , fixed point of extinction, unstable,
- $(K_1, 0)$ , fixed point of segregation, stable or superstable,
- $(0, K_2)$ , fixed point of segregation, stable or superstable,
- $(K_1, K_2)$ , fixed point of segregation (real or virtual), superstable,
- $(K_1, x_{2,a}^*)$ , fixed point of nonsegregation (real or virtual), unstable,
- $(K_1, x_{2,b}^*)$ , fixed point of nonsegregation (real or virtual), stable or unstable,
- $(x_{1,a}^*, K_2)$ , fixed point of nonsegregation (real or virtual), unstable,

$(x_{1,b}^*, K_2)$ , fixed point of nonsegregation (real or virtual), stable or unstable.

The explicit analytic expressions of the fixed points of nonsegregation, as well as their local stability analysis as a function of the parameters, are obtained as shown in [26] by using the one-dimensional first return map and also reported in the next section.

As already remarked in the Introduction, the goal of this paper is to investigate the role of the constraints, which are the values of  $K_1$  and  $K_2$ , when the two populations involved are characterized by some form of asymmetry such as  $\gamma_1 \neq \gamma_2$  or  $\tau_1 \neq \tau_2$  or  $N_1 \neq N_2$ . We recall that  $K_1$  and  $K_2$  represent the upper limit number of individuals of a population allowed to enter the system and, thus, represent possible regulatory policy choices.

In the next section, we shall describe several regions in the parameter plane  $(K_1, K_2)$  which lead to interesting dynamic behaviors, emphasizing on the differences with respect to the dynamics occurring in the symmetric case.

### 3. The Dynamics of the Model and Its Interpretation

In [26], we have analyzed the model of segregation and the effects of the entry constraints,  $K_1$  and  $K_2$ , for the peculiar case of two symmetric populations; that is,  $N_1 = N_2$ ,  $\gamma_1 = \gamma_2$ ,  $\tau_1 = \tau_2$ . In the current work, we investigate the case of asymmetric populations. In order to better compare the results, in our numerical simulations we keep the value of the parameters of population 1 as in [26]; that is

$$N_1 = 1.5, \quad \gamma_1 = 1, \quad \tau_1 = 4 \quad (11)$$

changing the values of the parameters of population 2. We start investigating the effects of the entry constraints assuming that population 2 differs from population 1 for a smaller number of members:

$$N_2 < N_1, \quad \gamma_2 = 1, \quad \tau_2 = 4. \quad (12)$$

We notice that although a few parameters are fixed, we shall describe the dynamic behaviors assuming  $N_2$ ,  $\gamma_2$ , and  $\tau_2$  at several different parameter constellations, keeping as goal the two-dimensional parameter plane  $(K_1, K_2)$ , and bifurcation structures similar to those illustrated and commented in this section have been obtained also when fixing different values for the parameters.

This asymmetric case is interesting as it is realistic to assume that the two groups allowed to enter a system are of different size. We can consider, as an example, the case of a city inhabited by natives and immigrants which both have to face the decision of living close to each other or not. The immigrants are usually less in number than the natives. As a first example, let us start analyzing the dynamics of the model for  $N_2 = 1.4$  and setting the entry constraints such that the largest population is more limited to enter the system with respect to the other population, assuming  $K_1 < K_2$ . For example, let us consider  $K_1 = 1.15$  and  $K_2 = 1.3$ . As shown in Figure 1(b), for this set of parameters we have

three stable equilibria: the equilibria of segregation  $(K_1, 0) \in \Omega_6 \cap D$  and  $(0, K_2) \in \Omega_4 \cap D$ , and one of nonsegregation  $(K_1, x_{2,b}^*) \in \Omega_5 \cap D$ . This last equilibrium and the unstable one  $(K_1, x_{2,a}^*) \in \Omega_5 \cap D$  are associated with the intersection of the reaction curve  $\phi_2$  with the straight line  $x_1 = K_1$  (see Figure 1(b)). These two equilibria exist because a specific constraint is imposed on the maximum number of members of population 1 allowed to enter the system (i.e.,  $K_1 = 1.15 < N_1$ ). As recalled in the previous section, each point of the region  $\Omega_5 \cap D$  is mapped in one iteration onto the straight line  $x_1 = K_1$ . The local stability of these two equilibria can be investigated considering the restriction of map  $T$  to  $x_1 = K_1$  for  $(K_1, x_2) \in \Omega_5 \cap D$ . The restriction of  $T$  to the invariant segment for  $0 \leq x_2 \leq x_{2,m}$ , where  $x_{2,m} = K_1 \tau_1 (1 - (K_1/N_1))$  is the maximum value belonging to  $\Omega_5 \cap D$ , is given by the one-dimensional map:

$$x_2(t+1) = f_2(x_2(t)),$$

$$f_2(x_2(t)) = \begin{cases} 0 & \text{if } F_2(K_1, x_2) \leq 0 \\ F_2(K_1, x_2) & \text{if } 0 \leq F_2(K_1, x_2) \leq K_2 \\ K_2 & \text{if } F_2(K_1, x_2) \geq K_2, \end{cases} \quad (13)$$

where

$$F_2(K_1, x_2) = x_2 \left[ 1 - \gamma_2 K_1 + \gamma_2 x_2 \tau_2 \left( 1 - \frac{x_2}{N_2} \right) \right]. \quad (14)$$

This one-dimensional map has three fixed points, shown in Figure 1(c). The point  $x_2 = 0$  corresponds to the fixed point  $(K_1, 0)$  of  $T$ . By straightforward calculations we can see that  $|d/dx_2 F_2(K_1, 0)| < 1$ , which implies that this fixed point is attracting in the direction of the line  $x_1 = K_1$  and it has a basin of attraction of positive measure. The nonzero fixed points internal to the range  $[0, x_{2,m}]$  are, thus, associated with the solutions of a quadratic equation, leading to

$$x_{2,b,a}^* = \frac{N_2}{2} \pm \sqrt{\left( \frac{N_2}{2} \right)^2 - \frac{K_1 N_2}{\tau_2}}. \quad (15)$$

These two fixed points of  $f_2(x_2(t))$  correspond to the fixed points  $P_a = (K_1, x_{2,a}^*)$  and  $P_b = (K_1, x_{2,b}^*)$  of the segregation model  $T$  and are the intersection points of the reaction curve  $\phi_2$  with the line  $x_1 = K_1$ . Calculating the value of the derivative of  $f_2(x_2(t))$  at the two equilibria, it is possible to determine whether they are locally stable or unstable, from which it follows the stability or instability of the fixed points  $P_a$  and  $P_b$  of  $T$ . It is worth remarking that the equilibria  $P_a$  and  $P_b$  belonging to  $\Omega_5 \cap D$  are present also in the symmetric case. However, in the symmetric case considered in [26] they are both unstable. This first difference has an important consequence. Indeed, it suggests that when the two populations have different size and so different level of tolerance (as for the specific form of the tolerance functions  $R_i$ , the population with a smaller number of members is also the less tolerant) it is possible to set the entry constraint only for the larger and more tolerant population, in our specific case population 1, to reduce the risk of segregation and to have a stable equilibrium of nonsegregation.

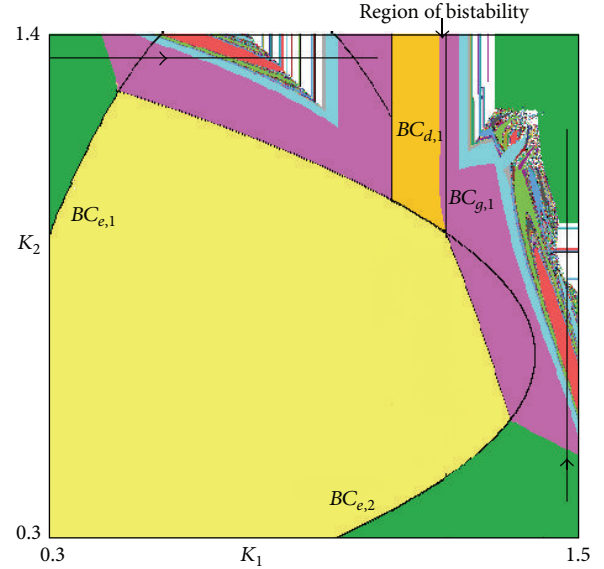


FIGURE 2: Two-dimensional bifurcation diagram on the  $(K_1, K_2)$ -parameter plane for map  $T$  at  $N_1 = 1.5$ ,  $N_2 = 1.4$ ,  $\tau_1 = \tau_2 = 4$ , and  $\gamma_1 = \gamma_2 = 1$ . Different colors are related to attracting cycles of different periods  $n \leq 30$ ; the white region corresponds either to chaotic attractors or to cycles of higher periods. In particular, the dark-green regions represent the set of values at which the equilibria of segregation are stable. For parameters in the yellow region besides the two equilibria of segregation there exists also the superstable fixed point  $(K_1, K_2)$ . For parameters in the orange region,  $(K_1, x_{2,b}^*)$  is a stable fixed point, coexisting with the two stable equilibria of segregation.

This first example highlights immediately a difference between the symmetric case and the asymmetric one considered here. To better understand the differences in the dynamics and the role of the entry constraints in the two situations, it is useful to observe the parameter space  $(K_1, K_2)$  in Figure 2. The stability region of the equilibrium  $(K_1, x_{2,b}^*)$  is the one colored in orange. This is a region in which this stable equilibrium of nonsegregation  $P_b$  coexists with the two stable equilibria of segregation (which are stable whatever the values of the entry constraints  $K_1$  and  $K_2$ ). An example of the related basins of attraction is shown in Figure 1(b). In Figure 2, the yellow region represents the set of values of the entry constraints for which the superstable equilibrium of nonsegregation  $P = (K_1, K_2) \in \Omega_7 \cap D$  exists. The curves  $BC_{e,1}$  and  $BC_{e,2}$  depicted on the figure represent the set of values of  $K_1$  and  $K_2$  for which the equilibrium  $(K_1, K_2)$  has a contact with the curves of nondifferentiability  $BC_{1,K}$  and  $BC_{2,K}$ , respectively, and, thus, represent curves at which the fixed point  $P$  undergoes a BCB. We have:

$$BC_{e,1} : K_2 = \tau_1 K_1 \left( 1 - \frac{K_1}{N_1} \right), \quad \text{where } F_1(K_1, K_2) = K_1, \quad (16)$$

$$BC_{e,2} : K_1 = \tau_2 K_2 \left( 1 - \frac{K_2}{N_2} \right), \quad \text{where } F_2(K_1, K_2) = K_2. \quad (17)$$

While the dark-green regions represent the values of the entry constraints for which only the two equilibria of segregation  $(K_1, 0)$  and  $(0, K_2)$  are stable, it is worth noting that this occurs either when both entry constraints are not stringent, that is,  $K_1$  takes values close to  $N_1$  and  $K_2$  takes values close to  $N_2$  (the green region in the upper-right corner of Figure 2), or when the entry constraints for one population are very stringent while the one for the other population is not stringent at all. For example, the dark-green region on the upper-left corner of Figure 2 represents the situation in which the members of population 1 are severely restricted to enter the system, while the members of population 2 are only marginally restricted to enter the system. In this case, the members of population 2 do not have problems to tolerate the small number of members of population 1 allowed to enter the system, but the members of population 1 do not tolerate the large presence of members of population 2 that are allowed to enter the system. This situation attracts more members of population 2 in the system and, at the same time, urges the members of population 1, which do not tolerate the growing number of members of population 2, to exit the system. This mechanism prevents the existence of an equilibrium of nonsegregation. Relaxing the entry constraint for population 1 (i.e., increasing the value of  $K_1$ ), we first have the appearance of a stable 2-cycle (a cycle of period two), the magenta region in Figure 2, and then, increasing further the value of  $K_1$ , a sequence of bifurcations from which stable cycles of any period appear, and also chaotic attractors, up to a region in which a 2-cycle is stable again. From this point, relaxing further the entry constraint for the members of population 1, it is possible to enter the orange region in Figure 2 associated with the existence of a stable equilibrium of nonsegregation. This is the sequence of bifurcations that occurs moving the parameters along the black horizontal arrow in Figure 2.

The appearance either of a stable cycle of nonsegregation or a stable nonsegregation equilibrium by relaxing the entry constraint for population 1 has a straightforward social explanation. Indeed, relaxing the entry constraint for population 1 we have more members of this population that can enter the system. This prevents the members of population 2 that are only marginally restricted or not restricted at all, to enter the system as they do not tolerate the larger and larger number of members of population 1 that are allowed to enter the system when  $K_1$  increases. It follows that a balancing effect prevails. Members of population 1 tolerate more the presence in the system of members of the other group and they would enter the system in a great number but are prevented to do so by the imposed entry constraint. At the same time, members of population 2, that can enter the system as they do not suffer or only partially suffer an entry constraint, do not enter the system in a massive way as they do not tolerate the larger presence of members of population 1 that are allowed to enter due to a relaxation of their entry constraint. As a result, the number of members that enter the system is limited for both the populations and this leads to a stable equilibrium of nonsegregation. This example suggests that, in order to have the coexistence of two different groups of people with a different level of tolerance toward each other in a system, an entry constraint on the more tolerant group has

to be imposed. This will partially reduce the presence of the members of the more tolerant population in the systems and as a consequence it will reduce the willingness of the members of the less tolerant population to leave the system. However, the entry constraint for the more tolerant population should not be too tight, as there is the risk to make the system too much attractive for the less tolerant population with the possibility to have a massive presence of its members which could lead to equilibria of segregation.

We can conclude that the entry constraints must be imposed in such a way to balance the entries of the two involved populations.

The possibility to have the equilibrium of nonsegregation  $P_b = (K_1, x_{2,b}^*) \in \Omega_5 \cap D$  stable represents one of the main differences between the symmetric and asymmetric cases. This region is represented in orange in Figure 2. This denotes that, to have a stable equilibrium of nonsegregation there, is the possibility to impose an entry constraint only on the larger population, which has to be fixed neither too stringent and nor too weak.

On the other hand, it is very interesting to note that not imposing or imposing very weak entry constraints to the larger population and at the same time imposing entry constraints on the smaller population, there is no possibility to converge to a stable equilibrium of nonsegregation. Note that the vertical arrow depicted in Figure 2 does not cross any yellow or orange region (the only regions that indicate the presence of stable equilibria of nonsegregation). This has a straightforward explanation related to the effect of limiting the entry to the members of the smaller and less tolerant population. In particular, imposing a stringent entry constraint on the less tolerant population and a relaxed entry constraint (or not imposing it at all) on the more tolerant population increases the risk of segregation mainly due to overshooting. Indeed, this leads to a situation in which many members of the more tolerant population enter the system attracted by the large and positive gap between the maximum tolerate number of members of the other group and their limited presence in the system imposed by the stringent entry constraint and members of the less tolerant population leave the system because the massive presence of the members of more tolerant population is much over the maximum tolerate number.

For the same reason, the dark-green region on the lower-right corner of the parameter space in Figure 2 is much larger than the dark-green region on the upper-left. It follows that it is more convenient to impose an entry constraint on the more tolerant population to avoid the risk of segregation. This is an interesting and surprising finding as it is common opinion that an entry constraint should be imposed on the less tolerant population to avoid segregation.

We have provided the intuition behind the existence and the stability of the nonsegregation equilibrium  $(K_1, x_{2,b}^*) \in \Omega_5 \cap D$ . Let us go further and try to understand through which bifurcation this nonsegregation equilibrium loses its stability; that is, let us identify the nature of the bifurcation curves that bound the orange region in Figure 2. We start analyzing the nature of the bifurcation occurring at the straight line that

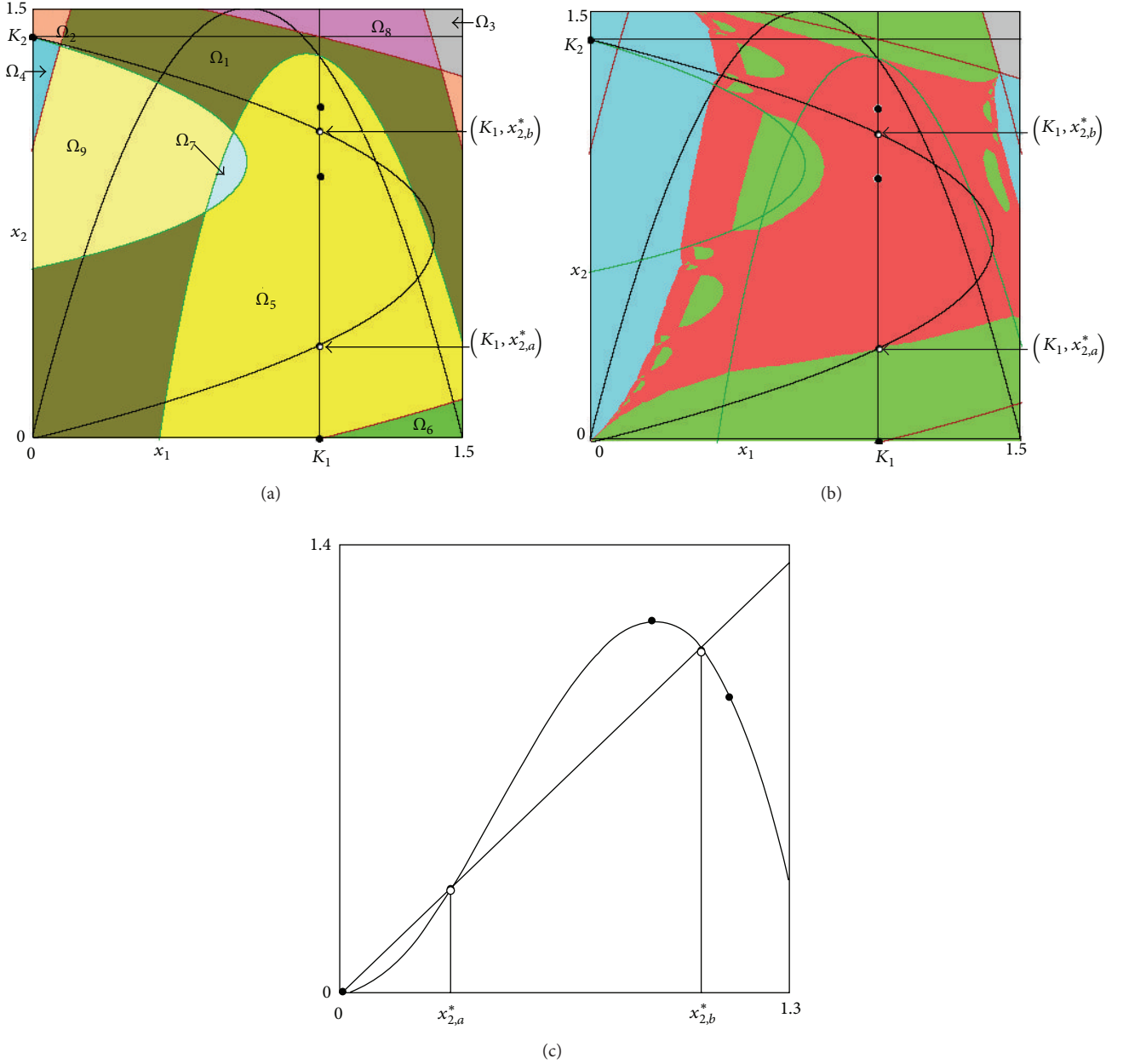


FIGURE 3: Parameters:  $N_1 = 1.5$ ,  $N_2 = 1.4$ ,  $\tau_1 = \tau_2 = 4$ ,  $\gamma_1 = \gamma_2 = 1$ ,  $K_1 = 1$ , and  $K_2 = 1.4$ . Panel (a), phase space divided in regions  $\Omega_i$ ,  $i = 1, \dots, 9$ . Panel (b), the green (resp., azure) region is the basin of attraction of the superstable equilibrium of segregation  $(K_1, 0)$  (resp.,  $(0, K_2)$ ), while the red region is the basin of attraction of the stable 2-cycle. In the first two Panels,  $BC_{1,K}$  and  $BC_{2,K}$  are the dark-green curves and  $BC_{1,0}$  and  $BC_{2,0}$  the dark-red curves, while  $\phi_1$  and  $\phi_2$  are the black curves. Panel (c), restriction of the map  $T$  on  $x_1 = K_1$  for  $x_2 \in [0, x_{2,m}]$ .

marks the left border of the orange region. Let us denote this bifurcation line as  $BC_{d,1}$ .

Comparing Figures 1 and 3, we can see that, as  $K_1$  is reduced from 1.5 to 1 and the line  $BC_{d,1}$  is crossed, moving from the orange region to the magenta region, the equilibrium  $(K_1, x_{2,b}^*)$  remains feasible; that is, it still belongs to the region  $\Omega_5 \cap D$ . As remarked above, the region  $\Omega_5 \cap D$  is degenerate as the entire region is mapped in one iteration on the line  $x_1 = K_1$ , so that each equilibrium in this

region must belong to  $x_1 = K_1$  and it has at least one zero eigenvalue. It follows that, to understand the destabilization of the equilibrium  $(K_1, x_{2,b}^*)$  crossing the bifurcation curve  $BC_{d,1}$  in the parameter space, it is sufficient to study the bifurcation that the fixed point  $x_{2,b}^*$  (given in (15)) of map  $f_2(x_2)$  undergoes for  $K_1$  crossing  $BC_{d,1}$ . By straightforward calculations it is easy to see that  $x_{2,b}^*$  loses its stability through a flip bifurcation occurring when  $K_1$  decreases, compare Figure 1(c) with Figure 3(c). It follows that the bifurcation



at which  $(K_1, x_{2,b}^*)$  from stable becomes unstable is obtained solving (from the definition of  $f_2(x_2)$  in (13))

$$\frac{d}{dx_2} F_2(K_1, x_{2,b}^*) = -1 \quad (18)$$

from which we obtain the bifurcation value:

$$\begin{aligned} \bar{K}_1 &= \frac{1}{8} (\gamma_2 \tau_2 N_2 - 8) \\ &+ \frac{1}{8} \sqrt{(\gamma_2 \tau_2 N_2 - 8)^2 + 32 \gamma_2^2 (\tau_2 N_2 \gamma_2 - 2)}. \end{aligned} \quad (19)$$

For  $K_1 < \bar{K}_1$  the equilibrium  $x_{2,b}^*$  (equivalently  $(K_1, x_{2,b}^*)$ ) is stable while for  $K_1 > \bar{K}_1$  the equilibrium loses its stability and a stable 2-cycle appears. It follows that the BCB curve at which  $(K_1, x_{2,b}^*)$  undergoes a nonsmooth period doubling (or flip) bifurcation (also shown in Figure 2) is the following:

$$BC_{d,1} : K_1 = \bar{K}_1. \quad (20)$$

Starting from a point in the orange region of the  $(K_1, K_2)$ -parameter space of Figure 2, where the nonsegregation equilibrium  $(K_1, x_{2,b}^*)$  is stable and feasible, decreasing  $K_1$  (i.e., making the entry constraint for population 1 more stringent) it loses stability via the bifurcation described here, crossing  $BC_{d,1}$ . However, we can see that another different bifurcation occurs as  $K_1$  is increased (relaxing this entry constraint). From Figure 3 we can also see that there exists a strip in which we have coexistence between the stable equilibrium of nonsegregation and a stable 2-cycle, also observable in Figure 4.

Let us first investigate the bifurcation leading to the appearance of this stable 2-cycle. From Figure 4(a) we observe that it is of the form  $\{(K_1, \bar{x}_2), T(K_1, \bar{x}_2)\}$  with  $(K_1, \bar{x}_2)$  belonging to the straight line  $x_1 = K_1$  inside the region  $\Omega_1 \cap D$ , while the other point  $T(K_1, \bar{x}_2)$  belongs to the region  $\Omega_5 \cap D$ . Thus, the periodic point  $(K_1, \bar{x}_2)$  of the 2-cycle is mapped in  $T(K_1, \bar{x}_2) = (F_1(K_1, \bar{x}_2), F_2(K_1, \bar{x}_2)) \in \Omega_5 \cap D$  and then a second iteration leads to the same point; that is,  $(K_1, \bar{x}_2) = T^2(K_1, \bar{x}_2) = (K_1, F_2(F_1(K_1, \bar{x}_2), F_2(K_1, \bar{x}_2))) = (K_1, G(x_2))$ . So the appearance of the 2-cycle can be investigated by use of the following one-dimensional first return map on  $x_1 = K_1$ :

$$\begin{aligned} x_2(t+1) &= G(x_2(t)) \\ &= F_2(K_1, F_2(F_1(K_1, \bar{x}_2), F_2(K_1, \bar{x}_2))) \end{aligned} \quad (21)$$

in the range  $x_{2,m} = K_1 \tau_1 (1 - (K_1/N_1)) < x_2 < K_2$ . This one-dimensional map is represented in Figure 4(c), see also an enlargement in Figure 4(d). This one-dimensional first return map shows that the stable 2-cycle appears via a *saddle-node BCB* together with another 2-cycle which is unstable. This is an interesting border-collision bifurcation which does not occur in the symmetric case analyzed in [26], marking another difference between the symmetric and asymmetric case.

It is worth remarking the situations depicted in Figure 4(c) (for the first return map of  $T$  on  $x_1 = K_1$ ) as well as in Figures 1(c) and 3(c) (for the restriction of  $T$  on  $x_1 = K_1$  when

$x_2 \in [0, x_{2,m}]$ ). The unstable fixed point of nonsegregation  $P_a = (K_1, x_{2,a}^*)$  marks the border of the basins of attraction between the stable fixed point of segregation  $(K_1, 0)$  and a different attracting set of nonsegregation. This underlines an interesting aspect of the entry-exit dynamics of the model. Indeed, it shows that when the presence of members of population 2 in the system at the current time  $t$  is small, specifically  $x_2(t) < x_{2,a}^*$ , all of them sooner or later will exit the system and the only possible scenario is the convergence to the fixed point of segregation  $(K_1, 0)$ . On the contrary, when their presence in the system is relatively large, that is,  $x_2(t) > x_{2,a}^*$ , their persistence in the system is ensured in the long period. Although the causes are different and mainly related to the myopic adaptive mechanism employed by agents, this phenomenon resembles the well-know demographic Allee effect in population dynamics, which indicates a decrease in population growth rate at low density; see for example, [27]. Clearly, a similar effect is observable on the line  $x_2 = K_2$ .

Increasing further the value of  $K_1$ , in other words relaxing the entry constraint for population 1, we have that the nonsegregation equilibrium  $(K_1, x_{2,b}^*)$  becomes virtual; that is, it undergoes a BCB crossing the boundary of its admissible region  $\Omega_5 \cap D$  and it is no longer an equilibrium point after the crossing (as the point enters the region  $\Omega_1 \cap D$ ), leaving the stable 2-cycle as unique nonsegregation attractor, see Figure 5. The equation of the border collision bifurcation curve at which the equilibrium  $(K_1, x_{2,b}^*)$  becomes virtual is given by  $(K_1, x_{2,b}^*) \in BC_{1,K}$  leading to

$$BC_{g,1} : x_{2,b}^* = K_1 \tau_1 \left(1 - \frac{K_1}{N_1}\right). \quad (22)$$

Below, we shall see a different bifurcation mechanism occurring at the right boundary of the orange region associated with the stability of the equilibrium  $(K_1, x_{2,b}^*)$ .

Further relaxing the entry constraint for population 1, the 2-cycle becomes unstable via nonsmooth period-doubling border collision bifurcation and the process is repeated. Via a sequence of similar bifurcations we observe the transition to a chaotic attractor for the map  $T$ . At a sufficient large value of  $K_1$  the chaotic attractor becomes a chaotic repeller via a contact bifurcation with the boundary of its basin of attraction. In Figure 6 it is shown the chaotic attractor quite close to the boundary of its basin, as the parameter  $K_1$  is close to the bifurcation value.

The bottom-border of the orange region of Figure 2 corresponds to another interesting border collision bifurcation which is worth analyzing. The equation of the bifurcation curve  $BC_{e,2}$  is given in (17). Starting from the orange region of Figure 2 and tightening the entry constraint for population 2, that is, decreasing  $K_2$ , the equilibrium  $(K_1, x_{2,b}^*)$  becomes virtual, it undergoes a border collision bifurcation reaching the boundary of the region  $\Omega_5 \cap D$ , but at the same bifurcation value the superstable equilibrium  $(K_1, K_2)$  becomes feasible entering region  $\Omega_7 \cap D$ . That is, crossing the curve  $BC_{e,2}$  separating the orange region (a stable equilibrium of nonsegregation exists) from the yellow one (the superstable equilibrium  $(K_1, K_2)$  exists), at the bifurcation value the two equilibria are merging:  $(K_1, x_{2,b}^*) = (K_1, K_2)$ .

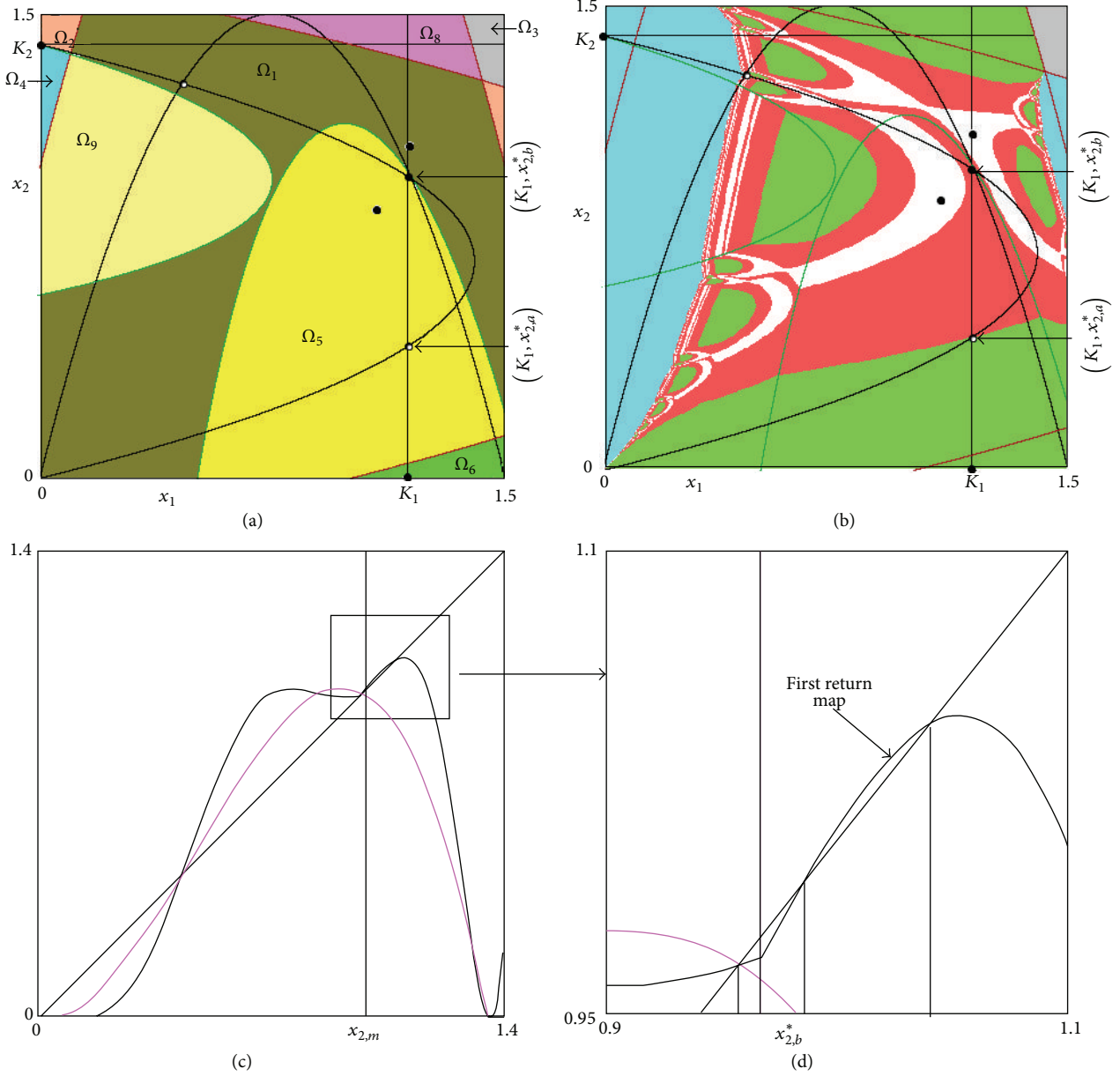


FIGURE 4: Parameters:  $N_1 = 1.5$ ,  $N_2 = 1.4$ ,  $\tau_1 = \tau_2 = 4$ ,  $\gamma_1 = \gamma_2 = 1$ ,  $K_1 = 1.19$ , and  $K_2 = 1.4$ . Panel (a), phase space divided in regions  $\Omega_i$ ,  $i = 1, \dots, 9$ . Panel (b), the green (resp., azure) region is the basin of attraction of the superstable equilibrium of segregation  $(K_1, 0)$  (resp.,  $(0, K_2)$ ), the red region is the basin of attraction of the equilibrium of nonsegregation  $(K_1, x_{2,b}^*)$  and the white region is the basin of attraction of the stable 2-cycle born through a nonsmooth saddle-node bifurcation. In the first two Panels,  $BC_{1,K}$  and  $BC_{2,K}$  are the dark-green curves and  $BC_{1,0}$  and  $BC_{2,0}$  the dark-red curves, while  $\phi_1$  and  $\phi_2$  are the black curves. Panel (c) shows the restriction of the map  $T$  on  $x_1 = K_1$  for  $x_2 \in [0, x_{2,m}]$  in pink and first return map  $G(x_2)$  in black. Panel (d) shows an enlargement of the picture in Panel (c).

The analysis performed up to now has shown the main nonsmooth bifurcations that can occur for  $N_2 = 1.4 < N_1$  (keeping fixed the values of the other parameters of the model as indicated in (11)-(12)). It is worth deepening the analysis of the dynamics of segregation for  $N_2 < 1.4$ . Reducing further the numerosity of population 2 and so reducing the tolerance of the members of this population toward members of the other population, we observe a clear enlargement of the orange region, comparing Figures 2 and 7. Moreover, the

nature of the bifurcation curve that marks the right border of the orange region changes for different values of  $N_2$ . Indeed, the right border of the orange region can represent either the moment in which  $(K_1, x_{2,b}^*)$  becomes virtual, exiting the region  $\Omega_5$ , as it is the case for  $N_2 = 1.4$  shown in Figure 2, or the moment in which  $(K_1, x_{2,b}^*)$  disappears through a *nonsmooth saddle-node bifurcation*. That is, the stable equilibrium  $(K_1, x_{2,b}^*)$  merges with the saddle  $(K_1, x_{2,a}^*)$  and both disappear. An example is shown in Figure 8, where in Figure 8(a)

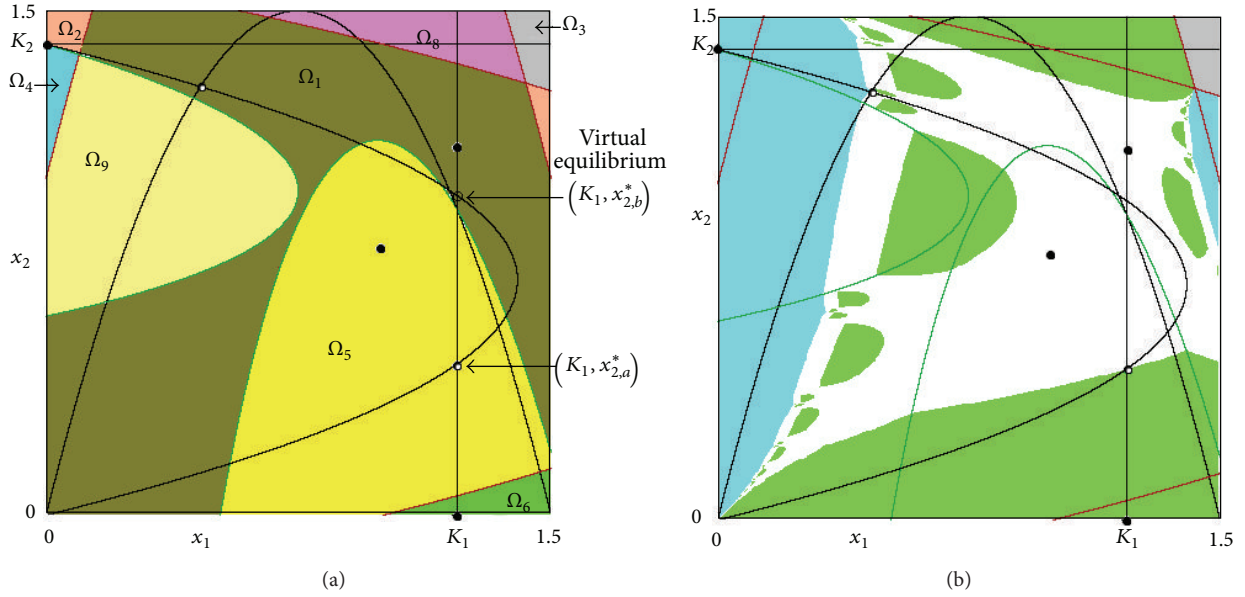


FIGURE 5: Parameters:  $N_1 = 1.5$ ,  $N_2 = 1.4$ ,  $\tau_1 = \tau_2 = 4$ ,  $\gamma_1 = \gamma_2 = 1$ ,  $K_1 = 1.22$ , and  $K_2 = 1.4$ . Panel (a), phase space divided in regions  $\Omega_i$ ,  $i = 1, \dots, 9$ . Panel (b), the green (resp., azure) region is the basin of attraction of the superstable equilibrium of segregation  $(K_1, 0)$  (resp.,  $(0, K_2)$ ), while the white region is the basin of attraction of the stable 2-cycle born through a nonsmooth saddle-node bifurcation. In these two Panels  $BC_{1,K}$  and  $BC_{2,K}$  are the dark-green curves and  $BC_{1,0}$  and  $BC_{2,0}$  the dark-red curves, while  $\phi_1$  and  $\phi_2$  are the black curves. The empty dot indicates the virtual equilibrium  $(K_1, x_{2,b}^*)$ .

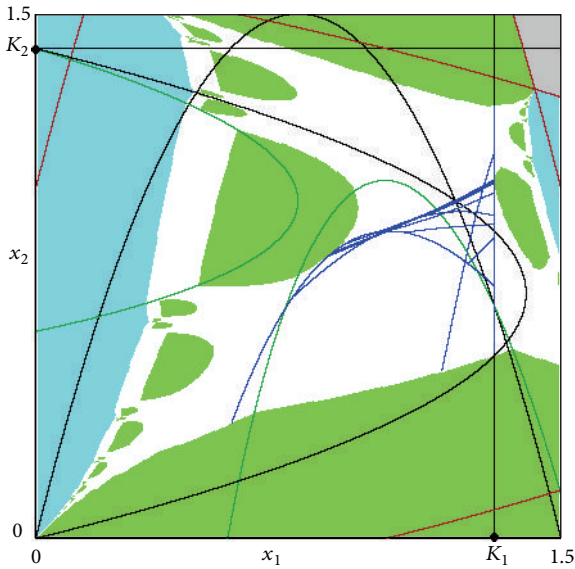


FIGURE 6: Parameters:  $N_1 = 1.5$ ,  $N_2 = 1.4$ ,  $\tau_1 = \tau_2 = 4$ ,  $\gamma_1 = \gamma_2 = 1$ ,  $K_1 = 1.31$ , and  $K_2 = 1.4$ . The green (resp., azure) region is the basin of attraction of the superstable equilibrium of segregation  $(K_1, 0)$  (resp.,  $(0, K_2)$ ), and the white region is the basin of attraction of the chaotic attractor depicted in blue.

the stable fixed point  $(K_1, x_{2,b}^*)$  coexists with a stable 2-period cycle and the two segregation fixed point and it is closed to the unstable fixed point  $(K_1, x_{2,a}^*)$ , while in Figure 8(b) fixed points  $(K_1, x_{2,b}^*)$  has disappeared after merging with  $(K_1, x_{2,b}^*)$

and the 2-period cycle has become the only stable attractor of nonsegregation. This bifurcation occurs when the reaction curve  $\phi(x_2)$  becomes tangent to the line  $x_1 = K_1$ , so that we get the following BCB curve:

$$BC_{h,1} : K_1 = \frac{1}{4} \tau_2 N_2 \quad \text{at which } K_1 = \max_{x_2} \{\phi(x_2)\}. \quad (23)$$

This bifurcation curve is reported at the right border of the orange regions in Figure 7 for  $N_2 = 1.3$  and  $N_2 = 1.2$ .

The social explanation for the enlargement of the orange region is straightforward. Reducing  $N_2$  makes population 2 less tolerant toward the presence of members of population 1, it follows that a consequence of limiting the entries in the system of the members of population 1 is to attract members of population 2 to enter the system. However, due to the limited tolerance, the members of population 2 do not enter the system in a massive way and this avoids problems of overshooting increasing the probability that the members of the two groups coordinates in an equilibrium of nonsegregation.

Another interesting difference occurring when the number of members of population 2 is smaller than the number of members of population 1 is the direct transition from the orange region to the green region, as it occurs in Figure 7(b) for  $N_2 = 1.2$ .

The numerosity of the members of the two populations involved in the system is not the only parameter of differentiation. We can have the two populations differing also in the parameters  $\gamma_1$  and  $\gamma_2$  which measure the propensity of the two populations to exit (enter) the system when the number of the members of the other population exceeds (is lower

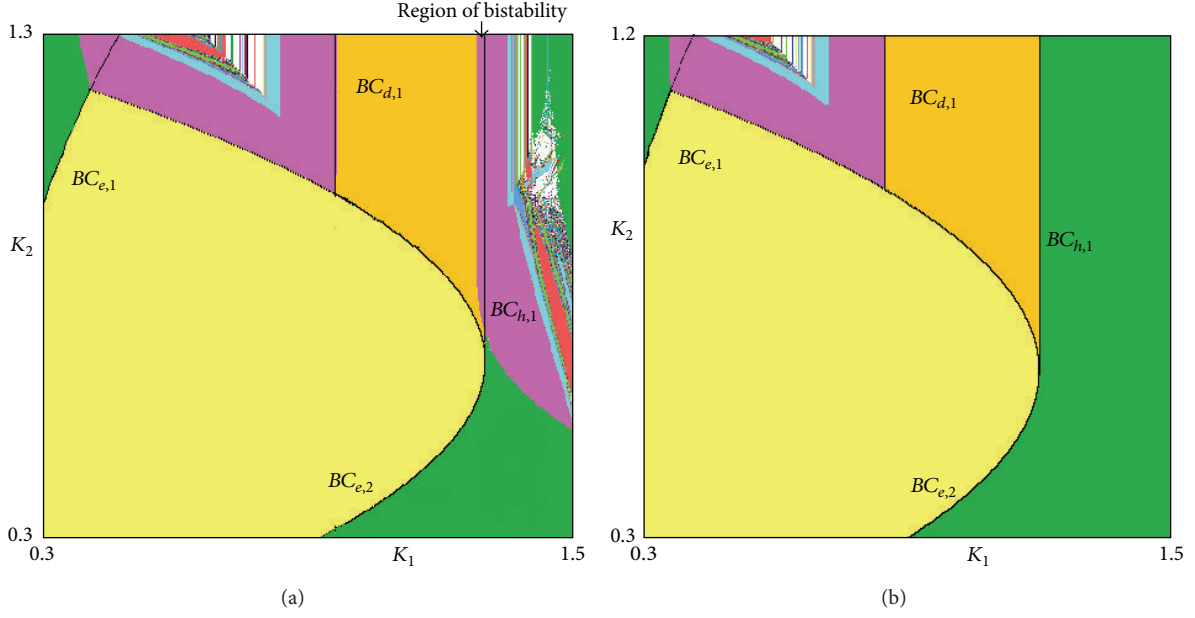


FIGURE 7: Two-dimensional bifurcation diagram in the  $(K_1, K_2)$ -parameter plane for map  $T$  at  $N_1 = 1.5$ ,  $\tau_1 = \tau_2 = 4$ , and  $\gamma_1 = \gamma_2 = 1$ . Panel (a)  $N_2 = 1.3$ . Panel (b)  $N_2 = 1.2$ . The meaning of the colored regions is as in Figure 2.

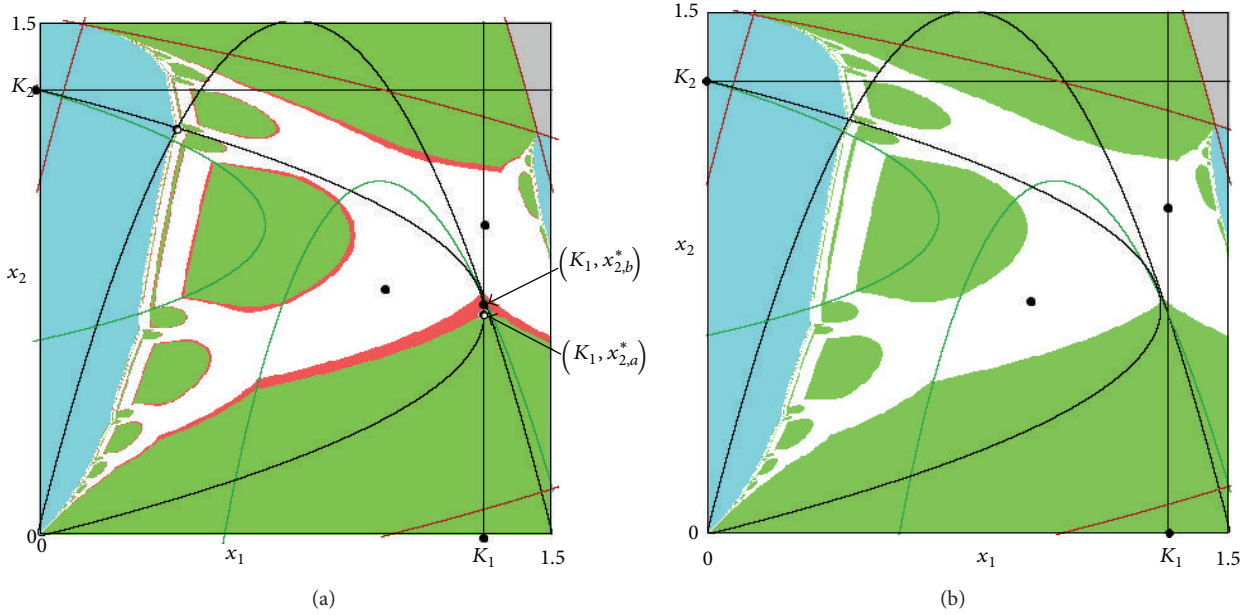


FIGURE 8: Parameters:  $N_1 = 1.5$ ,  $N_2 = 1.3$ ,  $\tau_1 = \tau_2 = 4$ ,  $\gamma_1 = \gamma_2 = 1$ ,  $K_2 = 1.3$ , and  $K_1 = 1.3$  in Panel (a),  $K_1 = 1.32$  in Panel (b). Green (resp., azure) region is the basin of attraction of the superstable equilibrium of segregation  $(K_1, 0)$  (resp.,  $(0, K_2)$ ), the red region is the basin of attraction of the nonsegregation equilibrium  $(K_1, x_{2,b}^*)$  and the white region is the basin of attraction of a stable 2-cycle.

than) the maximum level of tolerance. Let us assume that population 2 has numerosity  $N_2 = 1.2$ , as it is in Figure 7(b), and let us reduce the speed of adjustment for population 2; the value of  $\gamma_2$  reduces from 1 in Figure 7(b) to 0.5 in Figure 9(a). As expected, the slower reaction of population 2 to the overpresence (With overpresence of members of population-1 in the system, we mean a presence which exceeds the maximum

tolerated by the members of population-2 that are in a specific moment in the system.) of members of population 1 in the system increases the region of stability of the nonsegregation equilibrium  $(K_1, x_{2,b}^*)$ . The bifurcation curve  $BC_{d,1}$  moves to the left as  $\gamma_2$  decreases.

Comparing Figures 7(b) and 9(a) we can observe another interesting region in the parameter space  $(K_1, K_2)$  which



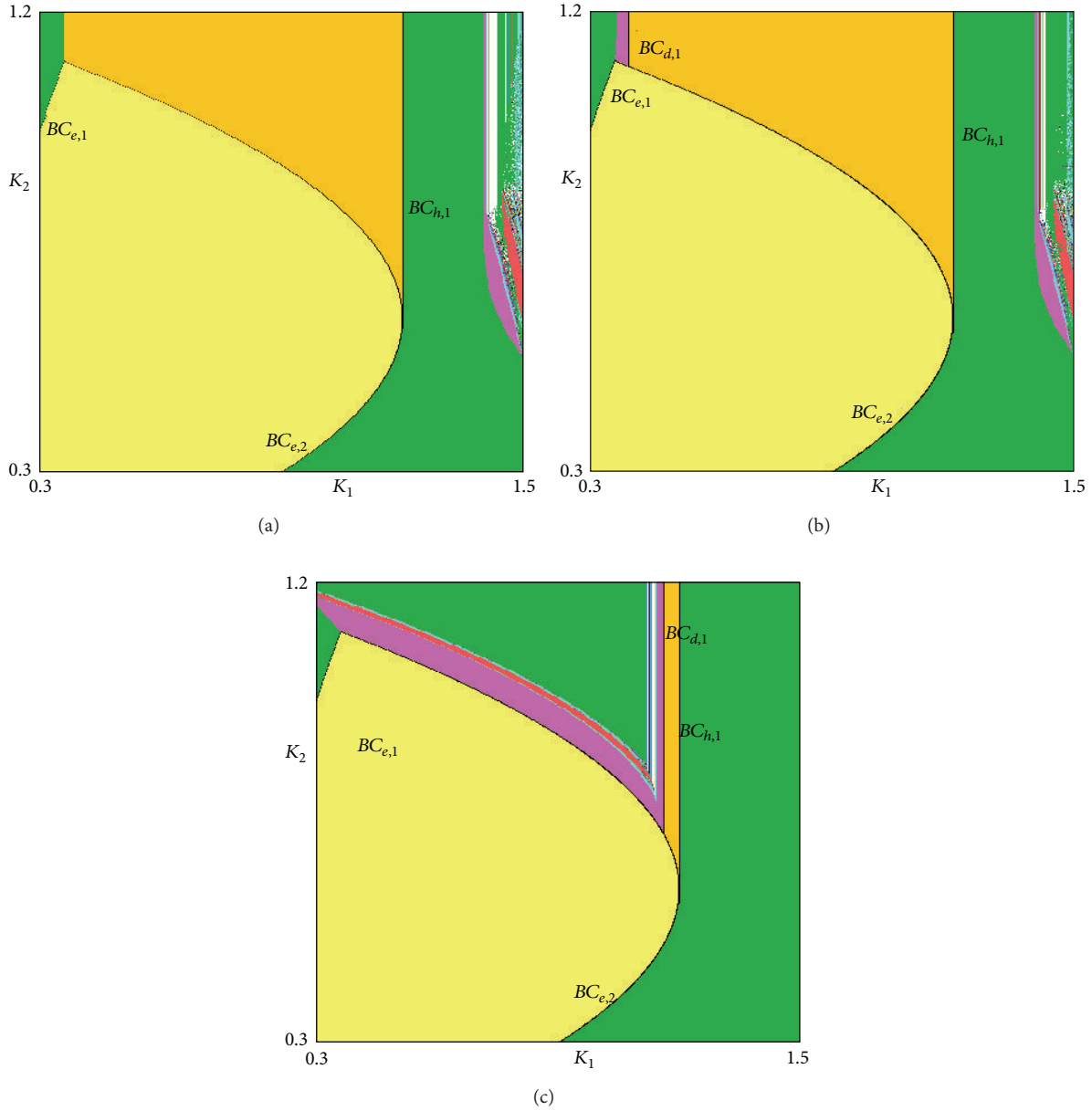


FIGURE 9: Two-dimensional bifurcation diagram on the  $(K_1, K_2)$ -parameter plane for map  $T$ . Parameters:  $N_1 = 1.5$ ,  $N_2 = 1.2$ ,  $\tau_1 = \tau_2 = 4$ , and  $\gamma_1 = 1$ . Panel (a)  $\gamma_2 = 0.5$ . Panel (b)  $\gamma_2 = 0.56$ . Panel (c)  $\gamma_2 = 4$ . Meaning of the colors of the regions as in Figure 2.

corresponds to the existence of a stable  $k$ -cycle of some period  $k$ . This is an attractor of nonsegregation, and it is interesting to observe that starting, for example, with  $K_2 = N_2$  and  $K_1 = N_1$ , the attractors of nonsegregation do not exist, but reducing  $K_1$  of a small amount we immediately observe the presence of a stable  $k$ -cycle as an attractor of nonsegregation. Reducing  $K_1$  further we first observe a situation in which only the two equilibria of segregation  $(K_1, 0)$  and  $(0, K_2)$  can be stable and for  $K_1$  even smaller we have the stable equilibrium of nonsegregation  $(K_1, x_{2,b}^*)$ . This strange transition reducing  $K_1$  is not trivial and easy to be explained. In fact, the nonsmooth bifurcations through which the stable cycles appear can be explained again using the first return map on  $x_1 = K_1$  in a way

similar to the one performed above. We skip here this analysis for the sake of simplicity, avoiding repetition of mechanisms.

It is easy to see that the speed of adjustment, parameters  $\gamma_1$  and  $\gamma_2$ , do not influence the stability region of  $(K_1, K_2)$  (the yellow region), indicating that it is always possible to fix the entry constraints in the two populations and have a stable  $(K_1, K_2)$  independently on the values of the speed of adjustments.

To complete the analysis on the effects of the asymmetries on the values of the parameters between the two populations involved, let us analyze the effect of the parameter  $\tau_2$  which measures the level of tolerance of population 2. It is worth to note that both parameters  $N_2$  and  $\tau_2$  influence the maximum

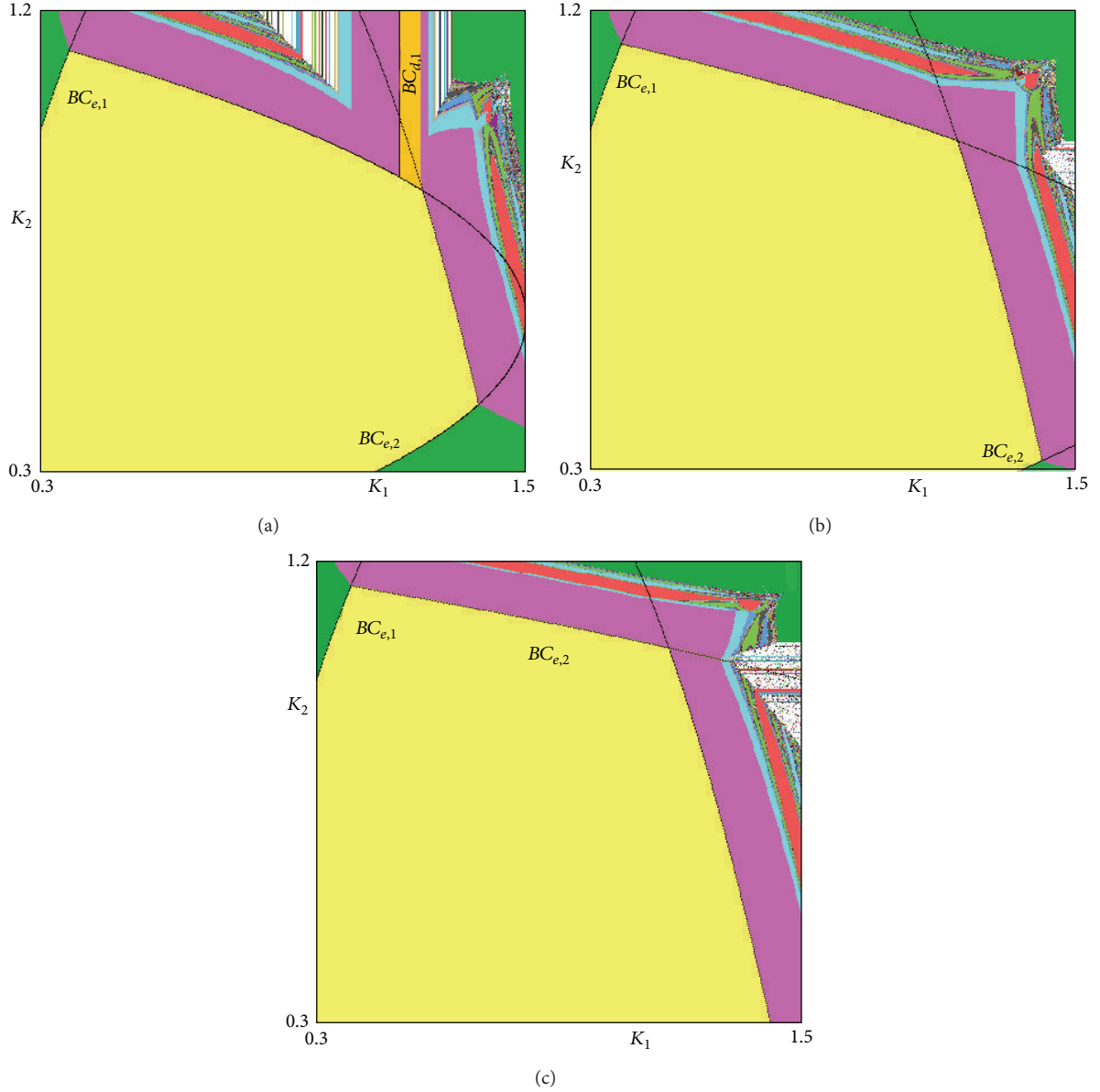


FIGURE 10: Two-dimensional bifurcation diagram on the  $(K_1, K_2)$ -parameter plane for map  $T$  at  $N_1 = 1.5$ ,  $N_2 = 1.2$ ,  $\tau_1 = 4$ , and  $\gamma_1 = \gamma_2 = 1$ . Panel (a)  $\tau_2 = 5$ . Panel (b)  $\tau_2 = 6$ . Panel (c)  $\tau_2 = 8$ . The meaning of the colors of the regions is as in Figure 2.

level of tolerance of population 2. However, parameter  $N_2$  has a double effect as it also influences the numerosity of population 2. Let us start fixing the values of the parameters of population 2 as in Figure 7(b); that is,  $N_2 = 1.2$ ,  $\tau_2 = 4$ , and  $\gamma_2 = 1$ . From this situation, let us increase the level of tolerance of population 2 up to  $\tau_2 = 5$ . Comparing Figures 7(b) and 10(a), it is possible to observe that an increase in the level of tolerance of population 2 leads to a larger yellow region, which means that the set of values of the entry constraints for which the equilibrium  $(K_1, K_2)$  is stable increases. However, at the same time it is possible to observe that as  $\tau_2$  changes from 4 to 5, that is, as population 2 becomes more tolerant, the orange region decreases in size. Moreover, the orange region disappears for  $\tau_2 = 6$  and  $\tau_2 = 8$ , see Figures 10(b) and 10(c).

This means that, as population 2 becomes more tolerant, the possibility to have an equilibrium of nonsegregation imposing entry constraint only on population 1, that is, for  $K_1 < N_1$  and  $K_2 = N_2$ , decreases to zero. Again, this phenomenon that may seem counter-intuitive is due to the overshooting problems explained above that threaten the existence of an equilibrium of nonsegregation. Nevertheless, considering the possibility to impose entry constraints on both populations, that is,  $K_1 < N_1$  and  $K_2 < N_2$ , when there is one population that it is more tolerant than the other, population 2 is more tolerant than population 1, the risk of segregation decreases (compare the three panels of Figure 10). Moreover, even these examples suggest once more that to avoid segregation it is more convenient to impose entry constraints to the more

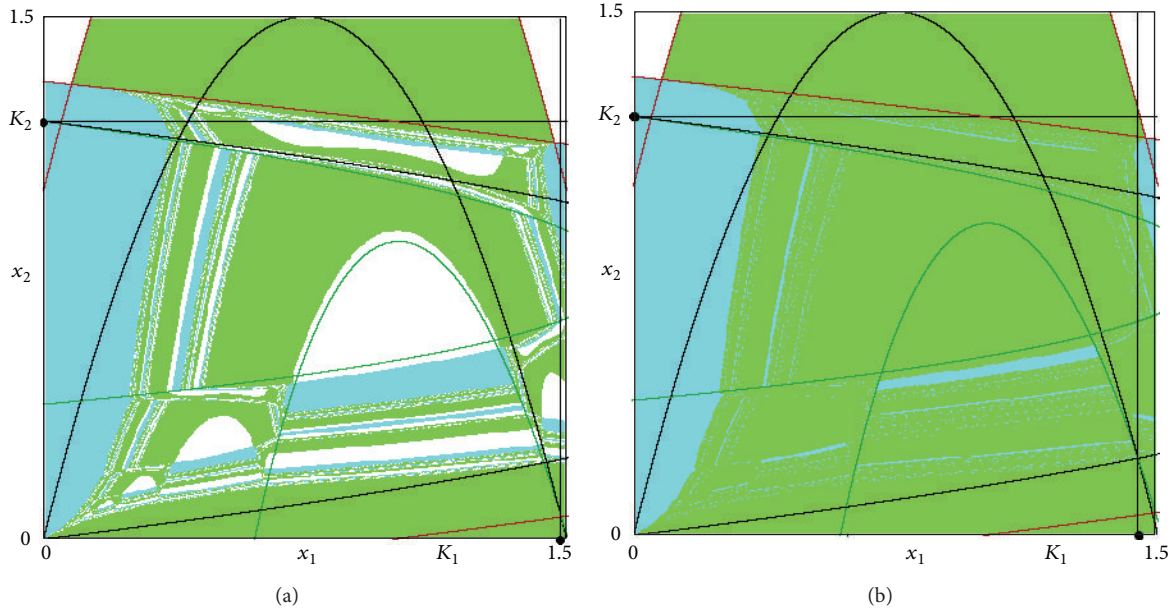


FIGURE 11: Parameters:  $N_1 = 1.5$ ,  $N_2 = 1.2$ ,  $\tau_1 = 4$ ,  $\tau_2 = 8$ ,  $\gamma_1 = \gamma_2 = 1$ , and  $K_2 = 1.2$ . Panel (a)  $K_1 = 1.48$ . Panel (b)  $K_1 = 1.44$ . The green (resp., azure) region is the basin of attraction of the superstable equilibrium of segregation  $(K_1, 0)$  (resp.,  $(0, K_2)$ ), the white region is the basin of attraction of the equilibrium of extinction  $(0, 0)$ .

tolerant population in order to curb the overshooting problems generated by massive waves of entries of members of the more tolerant population that risk to destabilize the coexistence.

Summarizing, the investigation reveals that differences in the level of tolerance between the two population involved increase the risk of overreaction between populations that could lead to segregation. The analysis provides nontrivial policy indications; that is, to avoid overshooting, and so segregation, a public authority has to impose stringent entry constraints to the more tolerant population.

Another interesting aspect is that the equilibrium  $(0, 0)$  is locally unstable, but due to the piecewise smooth definition of the map it attracts a set of points of positive measure in the phase plane. We have already shown the gray region in all the figures representing the phase plane (Figures 1(b), 3(a), 4(a), and 4(b), etc.). In all these cases, the gray region is always outside the rectangle  $D$  of interest, so that it plays no role. However, it may happen (depending on the parameters) that the gray region enters the rectangle  $D$ . This means the appearance of values for the two populations which lead to extinction. That is, all the members of the two populations can decide to exit the system, as shown for  $\tau_2 = 8$  in Figure 11(a) (where the color of the basin of the origin is set to white instead of gray to show it in better evidence).

The mechanism through which this occurs is quite simple to be explained. Due to the high level of tolerance of the two populations, with population 2 more tolerant than population 1, whenever the number of members of population 2 that are in the system is small these members decide to enter in a massive way in the system. The massive presence of the members of each population is highly nontolerated by the members of

the other population and this encourages all the members of each population to leave the system. This is a clear overshooting problem which paradoxically shows that two populations whose members have a high level of tolerance toward each others, with one group more tolerant than the other, are unable to self-adjust their entrance in the system in order to converge to an equilibrium of nonsegregation, but actually all of them leave the system.

It is worth noting that the basins of attraction of Figure 11(a) for  $K_1 = 1.48$  have a complicated structure. It is clearly visible the existence of parameter regions which are very sensitive to perturbations, so that it is difficult to predict whether the final state will be the survival of population 1 or 2 instead of extinction of both. The complex structure is related to the sequence of preimages. This can be seen observing that, for  $K_1 = 1.44$ , as in Figure 11(b), the system has only the two segregation points as unique attractors, and increasing  $K_1$  the white region in the upper right corner crosses the absorbing region  $D$ . Then, this small portion has infinitely many other preimages in  $D$  which lead to the structure observed in Figure 11(a).

#### 4. Conclusions

In this paper, we have analyzed the effectiveness of entry constraints to prevent segregation in a two-population model of adaptive dynamics as proposed in [4] where members of each group have a limited level of tolerance toward members of the other group. This work generalizes the results proposed in [26] for a symmetric setting to a nonsymmetric one, where the two populations involved differ in numerosity, maximum level of tolerance towards the others, and speed of

reaction to differences in the maximum tolerated number of the members of the other group and their effective presence in the system.

Our analysis reveals that the entry constraints can lead to a stable equilibrium of nonsegregation. In particular, the investigation underlines that to have an equilibrium of nonsegregation, a policymaker has to impose more stringent entry constraints on the more tolerant population in order to limit their willingness to enter the system and reduce the reaction to exit the less tolerant population. This study shows that the entry constraints can also be responsible for complicated dynamics that appears through different type of border collision bifurcations, such as stable cycles of different periods and chaotic attractors.

Further generalizations of the model are possible. In particular, it would be of interest to consider two different forms of the tolerance distribution  $R_i(x_i)$  for the two groups of people considered in the model. Indeed, as suggested by [1], different groups can have different forms of tolerance distributions although the linear representation of these distributions considered here represents a good approximation of the reality. Another interesting aspect that deserves to be analyzed is the evolution of the tolerance distributions of the groups as the result of the interaction of the members of the two groups in the system.

## Conflict of Interests

The authors declare that there is no conflict of interests regarding the publication of this paper.

## Acknowledgments

This work has been performed under the activities of the Marie Curie International Fellowship of Viktor Avrutin within the 7th European Community Framework Programme, the project “Multiple-discontinuity induced bifurcations in theory and applications.” The other two authors have worked under the auspices of COST Action IS1104 “The EU in the new complex geography of economic systems: models, tools and policy evaluation.”

## References

- [1] W. A. V. Clark, “Residential preferences and neighborhood racial segregation: a test of the schelling segregation model,” *Demography*, vol. 28, no. 1, pp. 1–19, 1991.
- [2] T. Baldwin and G. Rozenberg, “Britain “must scrap multiculturalism,”” *The Times*, 2004.
- [3] T. C. Schelling, “Models of segregation,” *The American Economic Review*, vol. 59, no. 2, pp. 488–493, 1969.
- [4] G. I. Bischi and U. Merlone, “An Adaptive dynamic model of segregation,” in *Nonlinear Economic Dynamics*, T. Puu and A. Panchuck, Eds., pp. 191–205, Nova Science Publisher, New York, NY, USA, 2011.
- [5] T. C. Schelling, “Dynamic models of segregation,” *Journal of Mathematical Sociology*, vol. 1, pp. 143–186, 1971.
- [6] J. M. Epstein and R. Axtell, *Growing Artificial Societies: Social Science from the Bottom Up*, MIT Press, Cambridge, Mass, USA, 1996.
- [7] P. R. Krugman, *The Self-Organizing Economy*, vol. 122, Blackwell, Cambridge, Mass, USA, 1996.
- [8] H. Wasserman and G. Yohe, “Segregation and the provision of spatially defined local public goods,” *The American Economist*, vol. 45, pp. 13–24, 2001.
- [9] I. Sushko, A. Agliari, and L. Gardini, “Bifurcation structure of parameter plane for a family of unimodal piecewise smooth maps: border-collision bifurcation curves,” *Chaos, Solitons and Fractals*, vol. 29, no. 3, pp. 756–770, 2006.
- [10] I. Sushko and L. Gardini, “Degenerate bifurcations and border collisions in piecewise smooth 1D and 2D Maps,” *International Journal of Bifurcation and Chaos in Applied Sciences and Engineering*, vol. 20, no. 7, pp. 2045–2070, 2010.
- [11] S. Brianzoni, E. Michetti, and I. Sushko, “Border collision bifurcations of superstable cycles in a one-dimensional piecewise smooth map,” *Mathematics and Computers in Simulation*, vol. 81, no. 1, pp. 52–61, 2010.
- [12] I. Sushko, L. Gardini, and K. Matsuyama, “Superstable credit cycles and U-sequence,” *Chaos Solitons & Fractals*, vol. 59, pp. 13–27, 2014.
- [13] Z. T. Zhusubaliyev and E. Mosekilde, *Bifurcations and Chaos in Piecewise-Smooth Dynamical Systems*, World Scientific, Singapore, 2003.
- [14] M. di Bernardo, C. J. Budd, A. R. Champneys, and P. Kowalczyk, *Piecewise-smooth Dynamical Systems: Theory and Applications*, Applied Mathematical Sciences, Springer, London, UK, 2007.
- [15] T. Puu and I. Sushko, *Business Cycle Dynamics, Models and Tools*, Springer, New York, NY, USA, 2006.
- [16] G. I. Bischi, C. Chiarella, M. Kopel, and F. Szidarovszky, *Nonlinear Oligopolies: Stability and Bifurcations*, Springer, Heidelberg, Germany, 2010.
- [17] R. H. Day, *Complex Economic Dynamics*, MIT Press, Cambridge, UK, 1994.
- [18] K. Matsuyama, *Good and Bad Investment: An Inquiry into the Causes of Credit Cycles*, Center for Mathematical Studies in Economics and Management Science Discussion Paper No.1335, Northwestern University, 2001.
- [19] L. Gardini, I. Sushko, and A. K. Naimzada, “Growing through chaotic intervals,” *Journal of Economic Theory*, vol. 143, no. 1, pp. 541–557, 2008.
- [20] W. Huang and R. Day, “Chaotically switching bear and bull markets: the derivation of stock price distributions from behavioral rules,” in *Nonlinear Dynamics and Evolutionary Economics*, R. Day and P. Chen, Eds., pp. 169–182, Oxford University Press, Oxford, UK, 1993.
- [21] F. Tramontana, F. Westerhoff, and L. Gardini, “On the complicated price dynamics of a simple one-dimensional discontinuous financial market model with heterogeneous interacting traders,” *Journal of Economic Behavior and Organization*, vol. 74, no. 3, pp. 187–205, 2010.
- [22] F. Tramontana, L. Gardini, and F. Westerhoff, “Heterogeneous speculators and asset price dynamics: further results from a one-dimensional discontinuous piecewise-linear model,” *Computational Economics*, vol. 38, no. 3, pp. 329–347, 2011.
- [23] G. I. Bischi, L. Gardini, and U. Merlone, “Impulsivity in binary choices and the emergence of periodicity,” *Discrete Dynamics in Nature and Society*, vol. 2009, Article ID 407913, 22 pages, 2009.



- [24] L. Gardini, U. Merlone, and F. Tramontana, "Inertia in binary choices: continuity breaking and big-bang bifurcation points," *Journal of Economic Behavior & Organization*, vol. 80, no. 1, pp. 153–167, 2011.
- [25] A. Dal Forno, L. Gardini, and U. Merlone, "Ternary choices in repeated games and border collision bifurcations," *Chaos, Solitons and Fractals*, vol. 45, no. 3, pp. 294–305, 2012.
- [26] D. Radi, L. Gardini, and V. Avrutin, "The role of constraints in a segregation model: the symmetric case," *Chaos, Solitons & Fractals*, vol. 66, pp. 103–199, 2014.
- [27] F. Courchamp, T. Clutton-Brock, and B. Grenfell, "Inverse density dependence and the Allee effect," *Trends in Ecology & Evolution*, vol. 14, no. 10, pp. 405–410, 1999.

